JOURNAL OF MATERIALS SCIENCE 31 (1996) 4111–4119

The processing of a magnesium-alumino-silicate matrix, SiC fibre glass-ceramic matrix composite using a pulsed Nd-YAG laser

Part I *Optimization of pulse parameters*

I. P. TUERSLEY, A. P. HOULT, I. R. PASHBY
Warwick Manufacturing Group, Department of Engineering, Warwick University, Coventry CV4 7AL, UK

As part of a continuing programme investigating the machining of various advanced composite systems, a study has been conducted using a 400 W pulsed Nd–YAG laser to process a glass-ceramic matrix composite comprising SiC fibres in a magnesium-alumino-silicate (MAS) matrix. The trials have been designed to permit a full comparison with results obtained from other ceramic composites, with a view to determining optimum lasing parameters for these and similar composite materials. The tests emphasize the influence of the fibre and matrix phase's ability to couple with the 1.06 μm laser emission. The fact that the MAS composition does absorb this energy to some extent, rather than relying entirely on conducted heat from the SiC fibres, has resulted in enhanced material removal rates and improved processed surface quality compared to, for instance, a borosilicate glass matrix material. Whilst the enhancement of either one of these criteria is generally made at the expense of the other, optimum parameters are identified and the resulting surface damage is assessed by electron microscopical examination.

1. Introduction

The wide-scale utilization of ceramic materials presents many attractive possibilities for a range of demanding engineering applications. They possess inherent properties such as high wear resistance, stiffness and specific strength, low susceptibility to environmental degradation and most significantly, the retention of these properties at elevated temperatures. These have been overshadowed by the problems encountered when their use is considered for actual components. A predominantly brittle mode of failure makes great demands on design and the very high hardness has limited methods of shaping the sintered product to expensive and time-consuming diamond grinding. The development of ceramic composite systems has addressed the problem of catastrophic failure with some success, but has, if anything, made efficient and flexible machining of the material even more necessary and yet more difficult.

Laser processing presents a potential solution. The process is non-contacting and therefore avoids the problems associated with tool wear and high contact forces between tool and workpiece. The use of CNC permits flexible geometries to be applied and the highly refractory nature of engineering ceramics suggests that they may be better suited than many materials to the extreme thermal conditions of material removal by vaporization.

This programme has already studied the processing characteristics of a SiC fibre, borosilicate glass matrix composite [1, 2] and now considers the effect of substituting a more refractory, crystallized glass matrix phase for the borosilicate. Tests have been conducted with a view to identifying the influence of the various laser-pulse parameters, and (in part II [3] of this publication) improving the processed surface quality by examining the effect of different process configurations.

2. Experimental procedure

2.1. Material

Tests have been conducted on plaques of glass-ceramic matrix composites (GCMC) consisting of continuous silicon carbide fibres in a magnesium-alumino-silicate (MAS) matrix. The fibre used was proprietary Nicalon 201™, filament-wound into unidirectional sheets. Twelve such sheets, when laid-up in alternate 0–90° layers and hot pressed, form a plaque 3.5–5 mm thick, and thicker or thinner plates may be fabricated by adjusting the number of plies accordingly.

The matrix was carefully compositionally tailored within the MgO–SiO_2–Al_2O_3 system, the major features of which are shown in the ternary phase diagram, Fig. 1. The exact choice of composition is

0022–2461

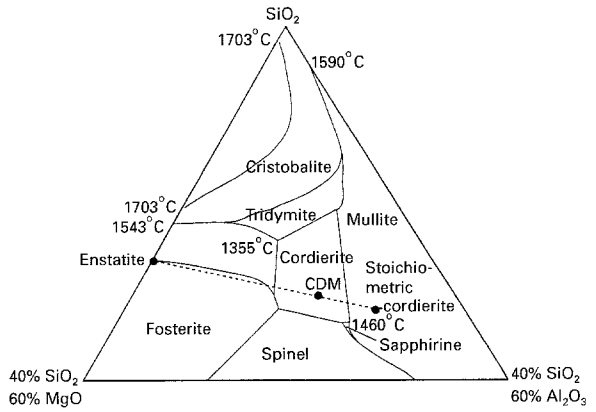

Figure 1 Ternary phase diagram for the system SiO_2–MgO–Al_2O_3. The matrix composition is shown on the cordierite–enstatite eutectic, marked CDM.

influenced by factors such as crystallization kinetics and stability of the resulting microstructure [4]. For instance, the glass-softening temperature and hot-pressing isotherm are optimized such that a fully crystallized matrix is produced without the processing temperature degrading the SiC fibres. This is achieved by the selection of off-stoichiometric silicate compositions, specifically near a eutectic between the primary phase cordierite and the binary silicate enstatite. This also presents the possibility of adjusting the thermal expansion, α, of the matrix with respect to the fibre [5]. Cordierite ($\alpha \sim 2.6 \times 10^{-6}$) in phase-mixture with enstatite ($\alpha \sim 8 \times 10^{-6}$) may cover a range from negative to positive values with respect to SiC (Nicalon $\alpha \sim 3.1 \times 10^{-6}$). The composition of the matrix phase in the material used in these tests is represented by the point "CDM" in Fig. 1.

The fibre content of the plaques has been measured at 30–35 vol%, but with local variations estimated to lie within the range 20–65 vol%. This relatively high degree of inhomogeneity occurs largely as a result of the manufacturing process route. As there is a significant difference in the thermal/mechanical properties of the matrix and the SiC fibre reinforcement, the large degree of variation in the localized fibre volume content may be assumed to be a major source of scatter in the process results, particularly material removal rate. This feature should, however, be regarded as a characteristic of this and similar materials.

2.2. Facilities and general laser configuration

All of the trial sets have been performed with the Lumonics JK701 Nd–YAG laser. The LD2 (low divergence) resonator arrangement has been used, the major performance characteristics of which are given in Table I. This was chosen because it permits the use of a high average power with tightly controlled beam divergence and therefore high intensity, essential for efficient penetration of these materials. An 80 mm focal length cemented achromat was used for the final stage lens. A water-cooled Coherent "Fieldmaster" external powermeter was used to verify the internal meter's reading or to evaluate the power losses occurring in the final optical stages.

TABLE I Performance of Lumonics JK701 Nd–YAG laser in LD2 configuration

Parameter	Range (LD2 resonator)
O/P wavelength	1060 μm
O/P energy (approx.)	0.5–15 J variable
O/P power (approx.)	Tuned cavity 230 W nom.
Repetition rate	17–200 Hz variable
Pulse duration	0.5–5 ms variable

A custom-built nozzle assembly was manufactured which facilitates nozzle alignment and allows rapid access to replace marked or damaged cover-glasses. It also permits full adjustment of the nozzle stand-off distance independently of focus position for trials involving changing the focal-point-to-surface distance, assist gas variations, etc. This has made adjustment of the laser set-up an easier task than would be required if the equipment were used for a standard industrial application.

Positioning of the workpiece was achieved by the use of a Unidex 400 CNC controller connected to a 3-axis workstation. This fully-programmable facility allows 600 mm × 600 mm × 300 mm of accurate and repeatable travel, facilitating the duplicating of test geometries on different specimens.

Initial tests identified nitrogen as a suitable assist gas in preference to oxygen or argon. This was manifolded to allow a maximum supply pressure of approximately 8 bar, measured from a point close to the nozzle orifice.

2.3. Test methodology

In order to attempt an optimization of the lasing parameters for this particular material, a systematic approach to the variation of test conditions has been adopted. A test programme was formulated that addresses the effect of varying the parameters individually (as far as is possible allowing for the interdependency of certain features of the pulse waveform). The effect upon material removal rate of varying the pulse energy, pulse duration and pulse intensity were investigated, and hence by implication, the peak power dependency according to the relation

$$\text{Peak power (kW)} = \frac{\text{Pulse energy (J)}}{\text{Pulse duration (ms)}} \quad (1)$$

In each parameter case, the penetrative power of the laser was assessed by drilling a single pulse, blind hole in the material. Having ascertained that the hole entry diameter and geometry are constant for a given beam expansion setting, the depth of the blind hole may be readily and accurately determined after sectioning the test piece, and may be assumed to be proportional to the volume of material removed. This also has the effect of isolating one of the laser parameters, the pulse repetition rate, from the analysis, as only a single shot is used.

3. Results and discussion

3.1. Laser processing results

3.1.1. Pulse duration variation

Six, individual single-pulse, blind holes were drilled for each of a range of pulse durations whilst maintaining a constant pulse energy. This was performed for pulse energies of 3.15, 7.25 and 14.5 J and the holes were then sectioned for analysis in the scanning electron microscope.

Fig. 2 is a graphical representation of the results, with the variation in pulse duration plotted against the depth of hole produced. Over the whole data set there is a general increase in the penetration of the plaque as the pulse duration is lengthened. The material removal efficiency exhibits a significant improvement as the pulse energy is increased from 3.15 to 7.2 J (compare the points as plotted between 2.00 and 3.00 ms, where the three data sets partially overlap) although there is less improvement as the energy is raised to 14.5 J. This suggest that of the two parameters, the pulse energy component of the peak power has the stronger influence on material removal.

Direct comparison with the results from the processing of the borosilicate GMC material [1] shows a marked increase in the penetrative capabilities of the laser with the MAS matrix composite. For a given set of lasing parameters, there is typically a 40%–50% increase in the depth of hole produced by a single shot, indicating a generally greater material removal efficiency achieved with this material.

3.1.2. Pulse energy variation

The pulse energy investigation was conducted in a similar manner, but with the pulse energy varied between its tuned limits at each of three pulse width values, 0.6, 1.5 and 5.0 ms. The resulting depth-of-hole measurements are plotted in Fig. 3. This shows an increase in penetration with greater pulse energy, the overall trend being quite gradual but with a slight irregularity in the case of the data points for a pulse duration of 1.5 ms which consistently produce a greater penetration than a similar pulse energy level but with a 5.0 ms pulse duration. There is generally less evidence of a "step change" in the results between the different pulse duration levels, however, and this confirms that the peak power is the major influence on the material removal.

3.1.3. Peak power variation

The variation of a single-pulse parameter, be it the energy or the duration, results in a corresponding change in the peak power of the laser pulse according to Equation 1. It is, therefore, of interest to consider the results of the preceding trials in terms of the penetration resulting from the variation in incident peak power instead of the "constituent" parameter. These trends are plotted in Figs 4 and 5.

Examination of Fig. 4 reveals two points of note. The data fall into three quite distinct groups, according to the three constant levels of pulse energy used for the trials. There is a significant improvement in the

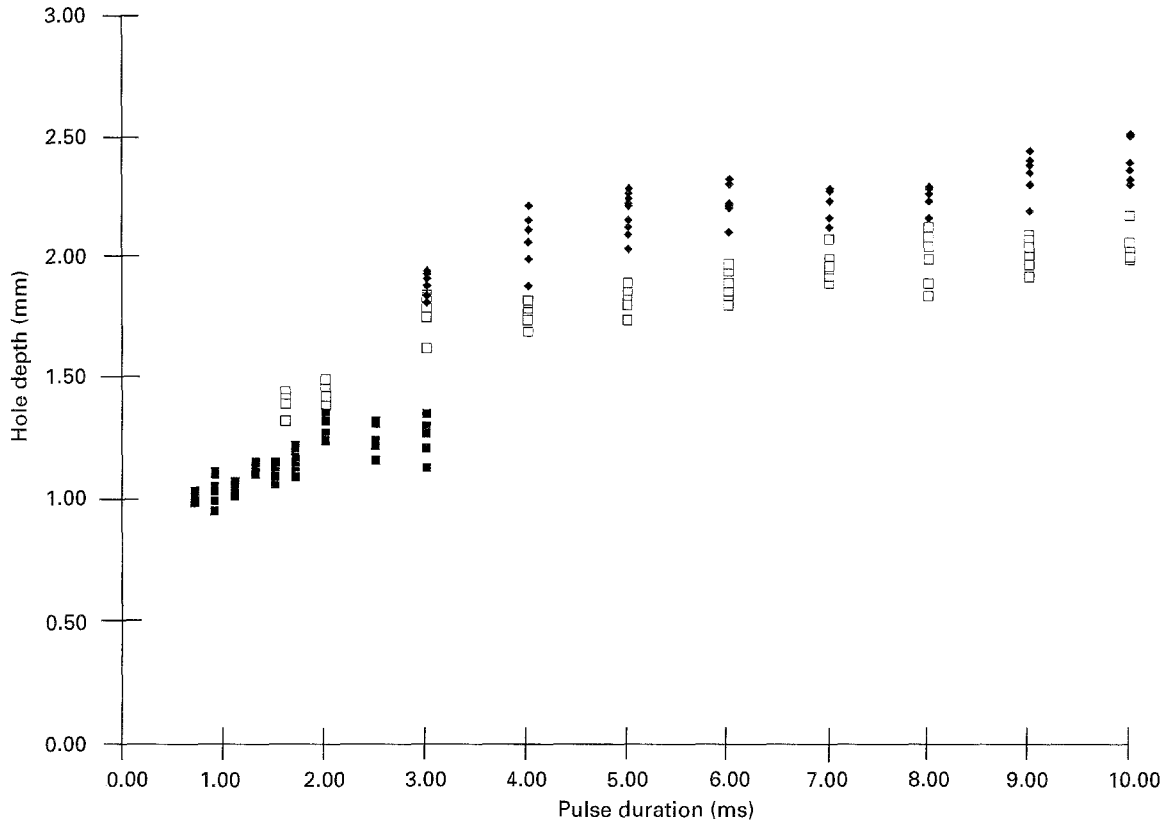

Figure 2 Effect of pulse duration, at constant pulse energies: (■) 3.15 J, (□) 7.2 J, (◆) 14.5 J.

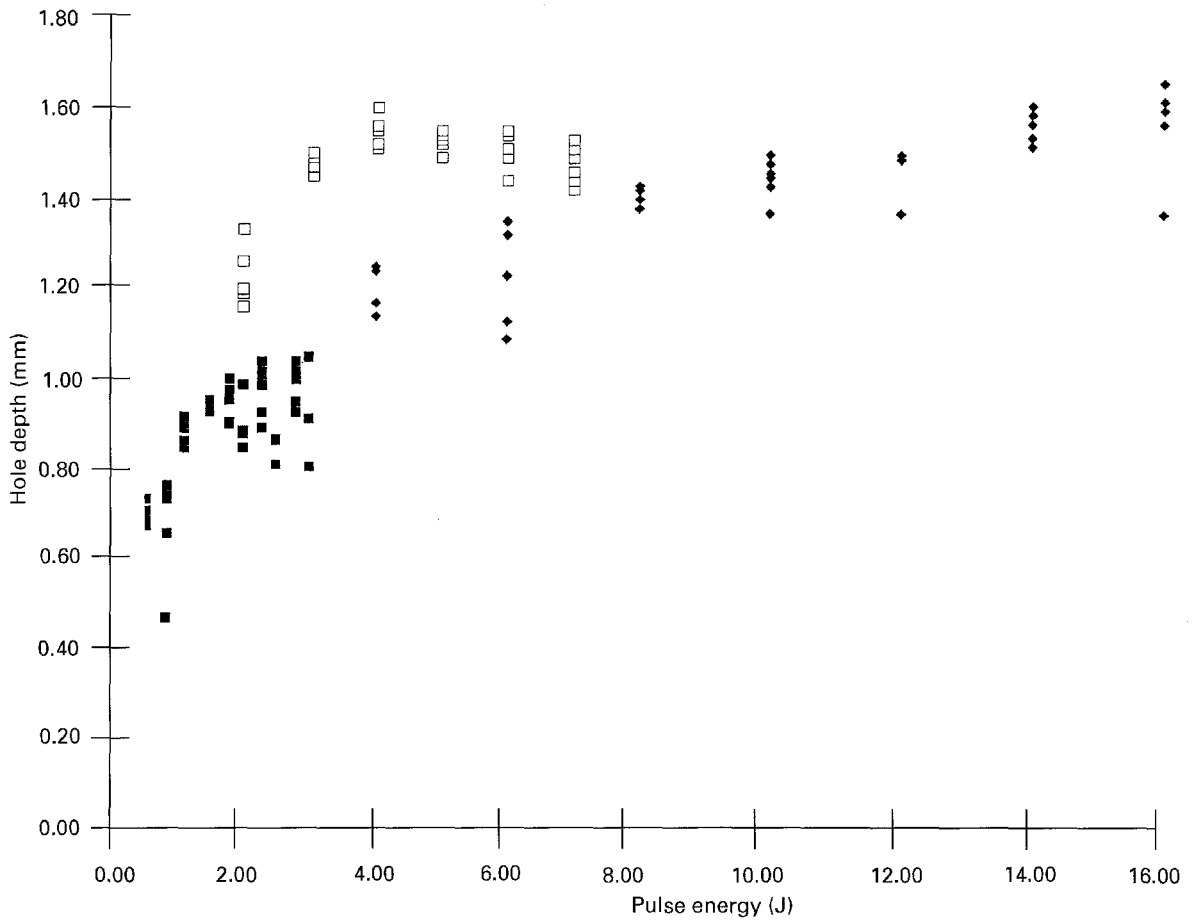

Figure 3 Effect of pulse energy, at constant pulse durations: (■) 0.6 ms, (□) 1.5 ms, (◆) 5.0 ms.

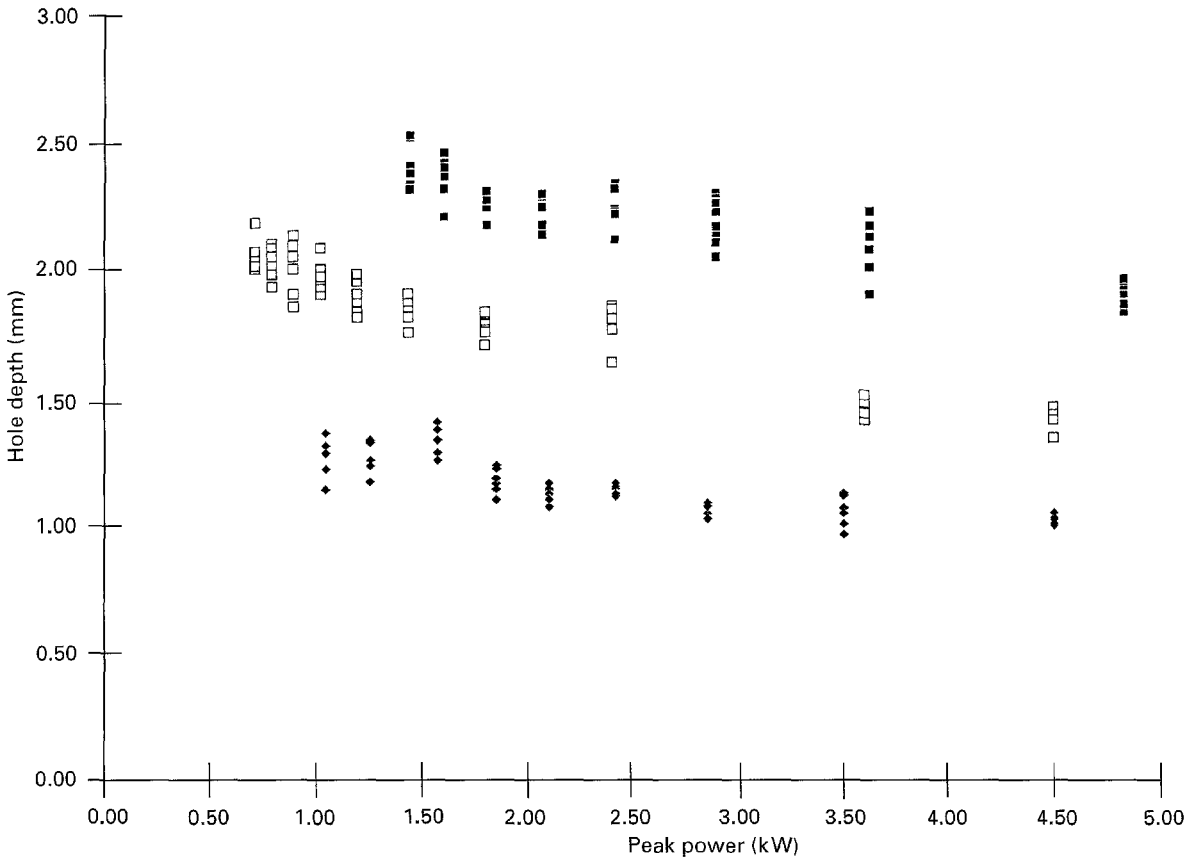

Figure 4 Peak power versus hole depth for various pulse durations: penetration at (■) 14.5 J, (□) 7.2 J and (◆) 3.15 J.

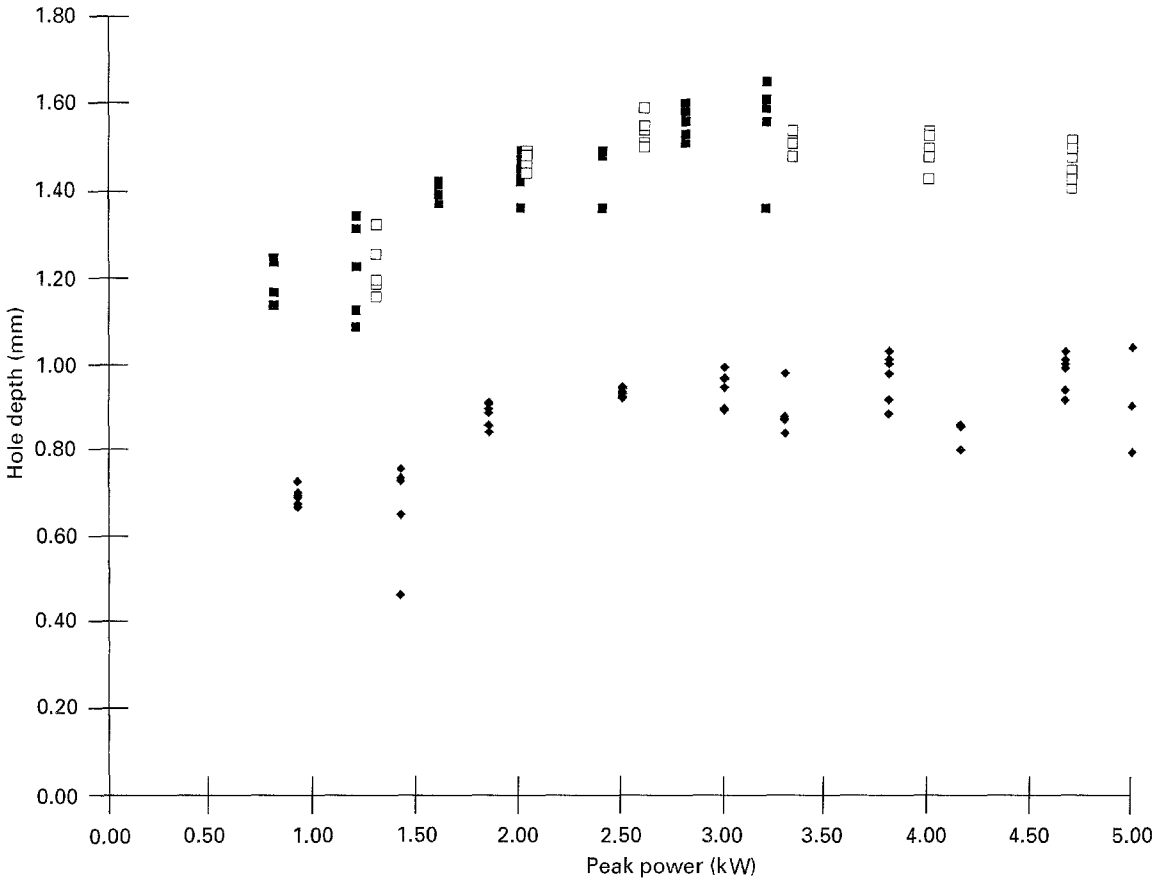

Figure 5 Peak power versus hole depth for various pulse energies: penetration at (■) 5.0 ms, (□) 1.5 ms, (◆) 0.6 ms.

penetration achieved with increasing pulse energy, for instance from ~ 1.00 mm to ~ 2.25 mm at 2.0 kW. Secondly, the data within each group show very little increase with increasing peak power (in fact there is a small decrease, especially at low peak powers, but this is generally not significant in comparison to the scatter in the data). This indicates that the penetration is increased by raising the pulse energy, but *not* significantly by increasing the pulse duration.

Fig. 5 confirms this conclusion. In this instance, the data may only really be separated into two groups, the results for pulse durations of 1.5 and 5.0 ms being very similar. There is generally a slight increase in hole depth as the peak power is increased as a result of raising the pulse energy, but little effect of increasing the pulse duration other than from the lowest levels.

3.1.4. Pulse intensity variation

As far as is permitted by the tuned operation of the laser, corresponding values for the laser parameters were used for the investigation of the affect of changing the beam intensity using the Beam Expansion Telescope (BET). This aids comparison between these results and those of the previous tests. The results are presented in Fig. 6, and confirm a result found in the tests on the GMC material. Once again, the three sets of data exhibit an inflexion in the individual lines-of-best-fit. The maxima (at which there is evidence of increased material removal efficiency) occur at a beam magnification of approximately 1.7, the minima at approximately 2.2, although this is less well defined. Both of these figures are broadly consistent with the previous findings. This inflexion has been noticed in similar trials on other materials [6], but the consistency of this result, irrespective of the material being processed, would suggest that it is a performance characteristic of the laser/optic train; it is possibly a consequence of the spherical aberration of the focus lens, or even due to the *spatial* (rather than temporal) distribution of the beam energy. Neither of these explanations may be readily verified, but the consistency of the result does suggest that there is an advantage in terms of material removal to conducting such trials at a beam magnification of approximately $\times$ 1.5–1.75.

3.1.5. Coupling of laser to MAS matrix phase

Comparisons made between the results of processing the MAS matrix material and those obtained from the "Pyrex" matrix GMC raise the question of the degree of influence of the two different matrices. It is known that borosilicate glasses are almost totally transparent to the YAG laser wavelength of 1.06 μm (for instance, [7]). However, as the MAS composition, unlike Pyrex, does not have applications as optical components, there are no published data on its optical properties. For this reason, monolithic samples of the two materials were obtained, and comparative trials of the material removal performed.

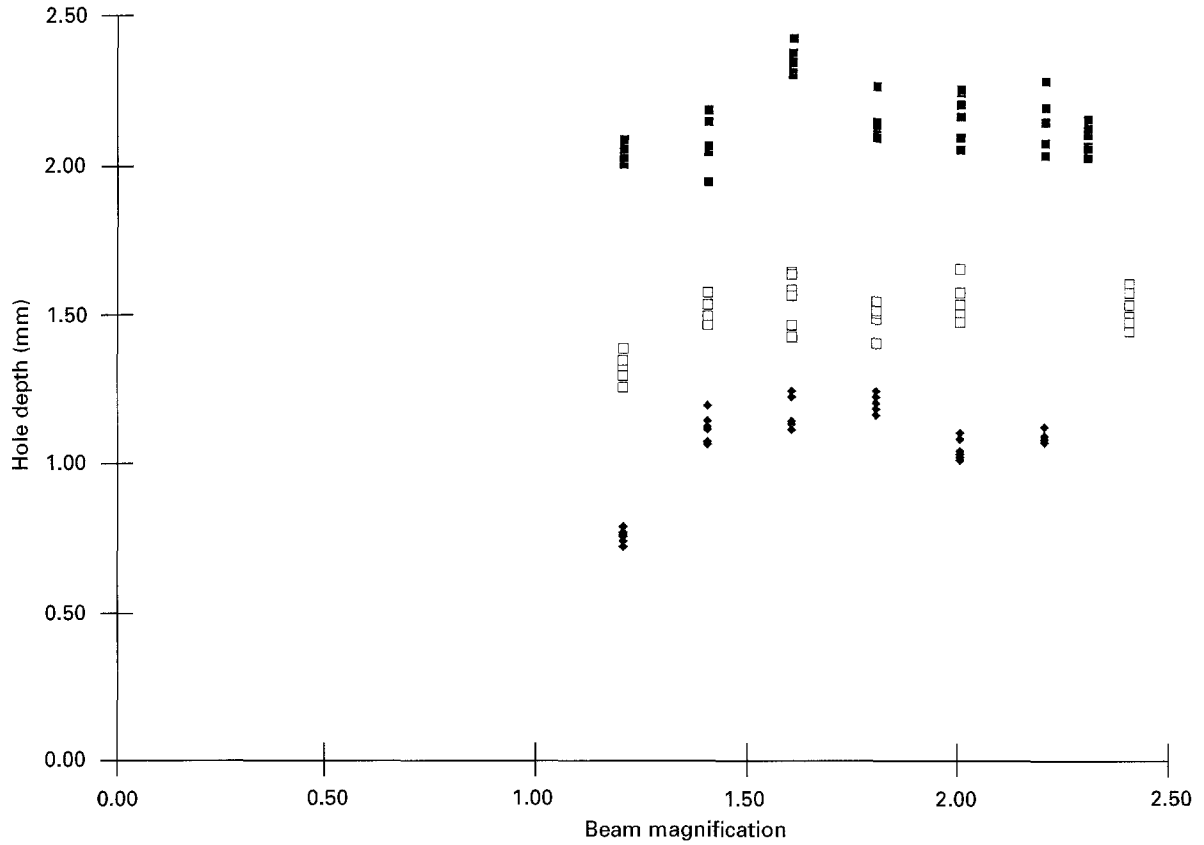

Figure 6 Effect of pulse intensity: (■) 15 J, 5 ms; (□) 7.2 J, 2 ms; (◆) 3.15 J, 0.9 ms.

Initially, samples of each material were subjected to single pulses of 3.1 J, 3.0 kW. The Pyrex showed no sign whatsoever of the incident laser beam, confirming that the material is indeed transparent to the YAG wavelength. The monolithic MAS, however, exhibited holes approximately 1.6 mm deep, similar in geometry to the holes produced in the composite. The low level of material redeposition on the bore of the hole was noted. The trials were repeated, but using a higher pulse energy of 15 J (whilst maintaining a peak power of 3.0 kW). This was sufficient to produce a through hole in the 2.2 mm thick MAS specimen with a single pulse. The Pyrex material still showed no signs of a melted hole, but produced a number of cracks radiating 5–6 mm from a central mark. It was concluded that at this power, impurities in the glass are heated by the laser. As the surrounding material remains unaffected, it is unable to accommodate the thermal expansion and/or shock and cracks in a brittle manner.

3.2. SEM examination and discussion of results

3.2.1. Material microstructure

Fig. 7 shows a backscattered electron image of the MAS-matrix composite microstructure. In this mode, the contrast levels detected result from the mean atomic number of the individual phases present; the higher the atomic number, the lighter the phase appears. The individual fibre sections and their dispersion through the matrix are clearly visible, giving an impression of the overall homogeneity. Within the matrix phase, there are occasional regions of *very* light contrast. These have been found to contain large traces of zirconium, and are present in the microstructure as impurities. The rest of the matrix exhibits a characteristic, mottled bi-phasic appearance, reflecting the two crystalline products of the tailored matrix composition, cordierite and enstatite. There is no evidence of preferential crystallization of either phase around the fibre/matrix interfaces.

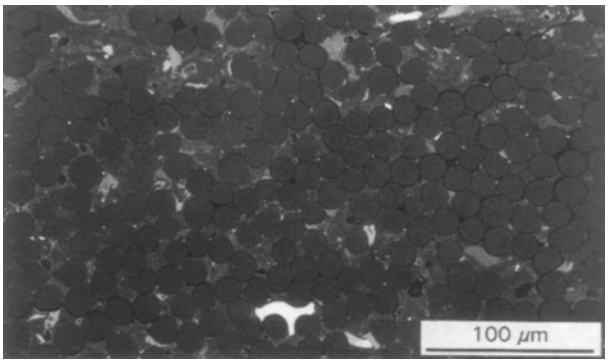

Figure 7 Backscattered electron image of the microstructure, showing general phase dispersion.

3.2.2. Experimental test results

The blind holes produced by each of the series of tests investigating the effects of varying the pulse duration, energy and intensity, were examined to determine any difference in the resulting hole geometry or extent of material damage.

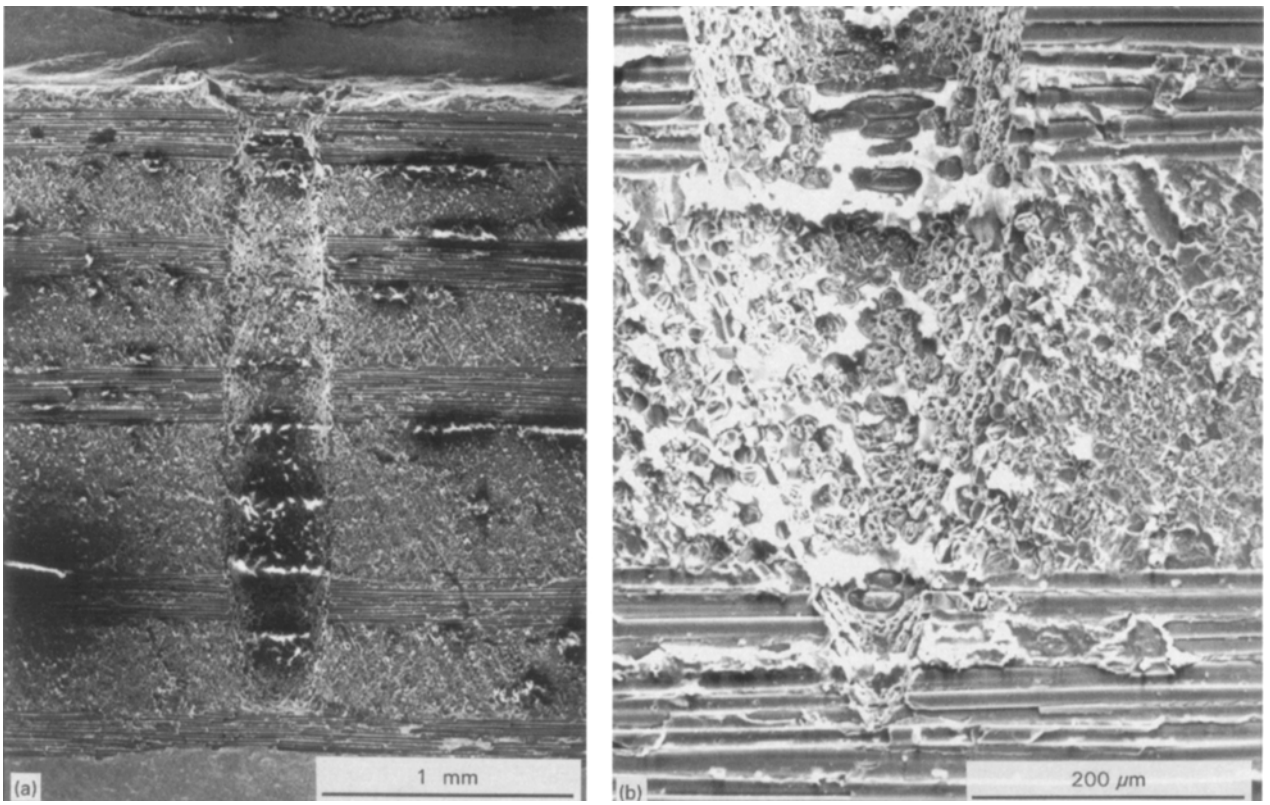

Figure 8 (a) Sectional geometry of deep-drilled holes, and (b) sharply pointed geometry at the extent of penetration.

The geometry of the holes is dependent upon the extent of the penetration. Shallow holes (up to approximately 500 μm deep) are convergently tapered, but subsequent penetration results in a parallel bore. Fig. 8a shows a typical deep-drilled blind hole from the series of tests investigating pulse duration effects.

One point of note when the hole geometries for the two materials are compared, is the profile of the bottom of the blind holes. In the trials on the GMC material [1], the bottom of the holes was invariably quite rounded; the holes produced in the MAS composite are *generally* more sharply pointed, in some cases very much so, as depicted in Fig. 8b. This may be due to variations in the spatial distribution of energy in the laser beam, but as the beam optic parameters are the same for the two sets of tests, this is unlikely. Measuring the beam's spatial energy profile is not a simple procedure, requiring special instrumentation, and this has not been addressed in this work. An alternative and more probable explanation to this observation is the relative conductive and absorptive characteristics of the respective matrix phases (the fibres being the same in each material).

It has been stated that the borosilicate glass matrix is almost completely transmissive of the 1.06 μm wavelength of the YAG laser, and that matrix vaporization is therefore almost entirely due to conduction of heat from the more absorptive SiC fibres. These, and other results in this work, indicate that the MAS matrix may be less transparent to the laser, resulting in a greater material removal efficiency of the composite as a whole and differences in the geometry of holes and kerfs. The pointed shape of the blind holes may therefore be a result of "primary" removal of the matrix, rather than "secondary", a result of heat conduction from the fibres. In this case the "vaporization front" could possibly assume the shape of the energy distribution across the diameter of the laser beam (which is ideally a Gaussian profile), rather than a more spherical, conduction-induced shape.

There is less evidence of redeposited material than was found with the GMC material, either on the surface around the entry hole or on the bore of the hole itself. This may be expected due to the more refractory nature of the matrix. The "countersink" feature found with the previous composite, where a region at the entry point showed depletion of the matrix and debonded fibres to a depth of about 200 μm and diameter up to 900 μm, is less marked, with a corresponding absence in most cases of the glass burr that had been noted before. Overall, the holes appear to be cleaner, but there are still traces of redeposited silicates, thermal spalling and microcracking. In Fig. 9 a region from the base of a typical blind hole is seen, showing the extent of these features. Note that the microcracking is not restricted to the matrix, but propagates through the fibres with very little evidence of crack deflection or branching. This may reflect the specific grade of fibre used to fabricate this material. Microstructural development of the composite performed as part of a separate research project has identified that the 201 grade of Nicalon fibre is not ideally suited to the temperatures experienced in the hot-pressing process. As well as governing the crystallization of the matrix, the processing temperature cycle is critical in determining the mechanical properties of the matrix/fibre interface. Measurements of the interface fracture energy, 2Γ, and the frictional shear

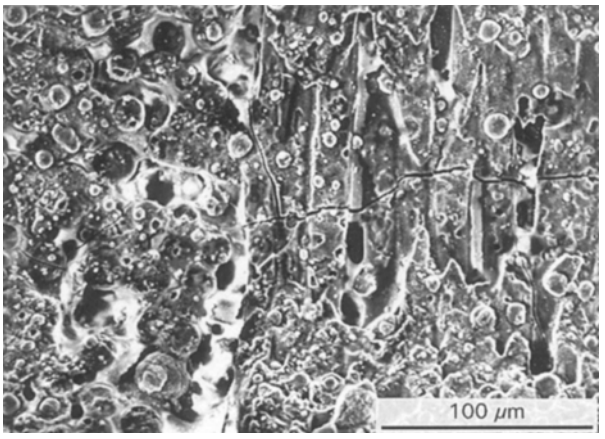

Figure 9 Material redeposition and microcracking on a processed surface.

stress, τ [8], show that thermochemical processing damage results in large fibre-clamping stresses, matrix craze cracking and an interfacial layer which generally too rigidly binds the fibre to the matrix. The use of an alternative grade, NL-607, was found to give improved results. The observations of Fig. 9 may therefore be explained, and more significantly, remedied, to some degree.

Fig. 10a and b show the extent of a heat-affected zone (H-AZ) in the holes. Showing the bore in section, Fig. 10a depicts a region 50–80 μm deep where there is evidence of matrix regression/debonding. This dimension varies according to the orientation of the fibre lay-up, as thermal conduction along the length of a fibre is greater than across fibres within a tow. The degree of debonding, shown in Fig. 10b may be attributable to a number of factors, but not least the difference in thermal expansion coefficients of the fibre and matrix. There is little evidence of damage to any greater depth, which compares well with the GMC material, which exhibited an H-AZ to a depth of 80 μm, but evidence of matrix modification as deep as 150 μm from the laser-processed surface.

4. Conclusion

The main area of interest in these tests is the influence that the pulse parameter adjustments have on the material removal rate. In common with the conclusions of the work on the glass matrix composite, the pulse parameter trials indicate that there is an increase in the material removal efficiency associated with increasing the incident peak power, and of the two parameters that influence the peak power level, it is the pulse energy rather than the pulse duration which makes the major contribution to this result. When compared with the glass matrix material, there is generally a 5%–10% increase in the material removal efficiency for any given set of laser pulse parameters. As the fibre reinforcing phase is the same in the two composites studied, this can be attributed to the different matrix compositions. The glass matrix (a borosilicate, nominally Pyrex) is known to be almost transparent to the wavelength emitted by a YAG laser, and vaporization and removal of this phase is therefore almost entirely due to conduction of heat from the fibres. In the case of the MAS matrix phase, the work performed on the monolithic samples proves that it does absorb a certain amount of the laser energy itself, although conduction is probably still a significant factor. As well as influencing the efficiency of the cutting process, the (partial) coupling of the laser beam to the matrix phase results in cleaner processed surfaces with greater dimensional consistency.

Acknowledgement

Financial support for this work, part of an investigation into the machining of advanced composites using traditional and laser techniques, has been gratefully

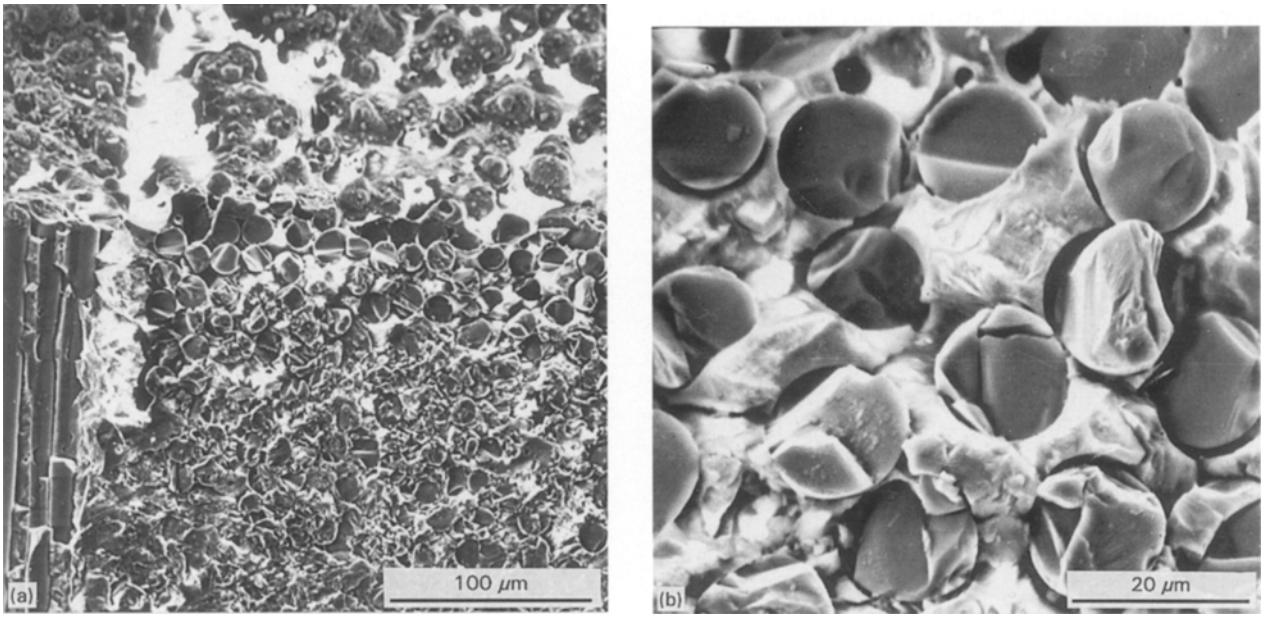

Figure 10 (a) Section of a hole, showing H-AZ, and (b) matrix/fibre debonding.

received from collaborating industrial partners and the UK DTI under the MTTMP programme.

References

1. I. P. TUERSLEY, A. P. HOULT and I. R. PASHBY, *J. Am. Ceram. Soc.* (1994) submitted.
2. *Idem, ibid.*
3. *Idem, ibid, Part II.*
4. M. H. LEWIS, A. CHAMBERLAIN, A. M. DANIEL, M. W. PHARAOH, A. G. RAZZELL and S. SUTHERLAND, "Microstructure and Macromechanical Behaviour of CMCs" in Progress of AGARD/NATO Workshop on Introduction of Ceramics into Aerospace Structural Composites, April 1993, Antalya, Turkey. NATO, No. AGARD-R-795.
5. M. H. LEWIS, A. M. DANIEL, A. CHAMBERLAIN, M. W. PHARAOH and M. G. CAIN, *J. Microsc.* **169** (2) (1993) 109.
6. A. MATSUNAWA, H. YOSHIDA and S. KATAYAMA, in "Proceedings of ICALEO '84", Vol. 44, "Materials Processing", (Laser Institute of America, Boston, USA, 1984) pp. 35–42.
7. MELLES GRIOT Inc., "Optics Guide 5" (1990) p. 3.13.
8. A. CHAMBERLAIN, M. W. PHARAOH and M. H. LEWIS, "Novel silicate matrices for fibre reinforced ceramics," in Ceramic Engineering and Science Proceedings, Cocoa Beach, Florida, Jan. 10-15th, 1993, Vol. 14, (Am. Ceram. Soc., 1993) pp. 939–946.

Received 23 September 1994
and accepted 9 November 1995